Published in IET Systems Biology
Received on 3rd June 2007
Revised on 27th October 2007
doi: 10.1049/iet-syb:20070029

ISSN 1751-8849

Modelling the influence of activation-induced apoptosis of CD4$^+$ and CD8$^+$ T-cells on the immune system response of a HIV-infected patient

G.-B. Stan[1] F. Belmudes[2] R. Fonteneau[2] F. Zeggwagh[3] M.-A. Lefebvre[3] C. Michelet[4] D. Ernst[2]

[1]*Control Group, Department of Engineering, University of Cambridge, Trumpington Street, Cambridge CB2 1PZ, UK*
[2]*Department of Electrical Engineering and Computer Science, University of Liège, B-4000 Liège, Belgium*
[3]*Supélec-IETR, Hybrid Systems Control Group, Rennes, France*
[4]*Clinique des Maladies Infectieuses, Unité de Pharmacologie Clinique and Laboratoire de Bactériologie-Virologie, Hôpital Pontchaillou, Rennes, France*
E-mail: gvs22@eng.cam.ac.uk

Abstract: On the basis of the human immunodeficiency virus (HIV) infection dynamics model proposed by Adams, the authors propose an extended model that aims at incorporating the influence of activation-induced apoptosis of CD4$^+$ and CD8$^+$ T-cells on the immune system response of HIV-infected patients. Through this model, the authors study the influence of this phenomenon on the time evolution of specific cell populations such as plasma concentrations of HIV copies, or blood concentrations of CD4$^+$ and CD8$^+$ T-cells. In particular, this study shows that depending on its intensity, the apoptosis phenomenon can either favour or mitigate the long-term evolution of the HIV infection.

1 Introduction

The human immunodeficiency virus (HIV) is a retrovirus that may lead to the lethal acquired immune deficiency Syndrome (AIDS). After initial contact and inclusion of the HIV particle into specific types of cell of the immune system, there is a cascade of intracellular events leading to the production of massive numbers of new viral copies, the death of infected cells and ultimately the devastation of the immune system.

Since the first identification of the disease in 1981, intensive studies have been carried out to understand the fundamental HIV infection mechanisms. HIV primarily infects cells of the human immune system such as helper T-cells (specifically CD4$^+$ T-cells), macrophages and dendritic cells. When the number of CD4$^+$ T-cells declines below a critical level, cell-mediated immunity is lost, and the body becomes progressively more susceptible to opportunistic infections. Progression from HIV infection to AIDS is primarily due to an extensive depletion of CD4$^+$ T-cells. Cell-mediated immunity is an immune response that does not involve antibodies but rather involves the activation of macrophages, natural killer cells, antigen-specific cytotoxic T-lymphocytes and the release of various cytokines in response to an antigen.

Several mechanisms are involved in the loss of CD4$^+$ T-cells and this topic is one of the most controversial issues in recent AIDS research. T-cell loss may be a consequence of direct destruction by the virus (direct virus-induced cytolysis) or of a defective T-cell generation. In 1991, apoptosis, also called programmed cell death, has been suggested as another mechanism responsible for T-cell depletion during the evolution of HIV-1 infection and an extensive body of recent literature is supporting this

hypothesis [1–5]. In HIV-infected patients, both infected and uninfected cells undergo accelerated apoptosis but, remarkably, the vast majority of the cells that undergo apoptosis are uninfected [6]. Furthermore, the level of apoptosis in HIV-1 infected patients is correlated to the levels of circulating $CD4^+$ T-cells and the stage of disease [6], which reinforces the idea that apoptosis induced by the HIV infection plays an important role in the death of the lymphocytes.

Mathematical analysis of the HIV/AIDS infection has been actively studied since the middle of the 1990's. Several authors have proposed mathematical models to describe the HIV infection dynamics [7–12]. These models are often represented by a set of nonlinear ordinary differential equations (ODEs) which model the long-term interaction between the immune system and the virus. They generally take into consideration several biological phenomena that influence the infection process, but, to the best of our knowledge, no mathematical model has yet tried to explain the influence of the activation-induced apoptosis phenomenon on the HIV infection dynamics.

In this paper, we propose a modification of the model proposed by Adams *et al.* in [7]. This modification aims at modelling the activation-induced apoptosis phenomenon and at analysing its influence on the HIV infection dynamics. Similar to the model initially proposed by Adams *et al.*, our model is characterised by different equilibrium points and does not directly aim at predicting the long-term collapse of the immune system, which may be due to several factors such as virus mutations or fatigue of the immune system resulting in progressive thymus degradation.

The paper is organised as follows. Section 2 introduces our proposed mathematical model for the influence of apoptosis on the HIV infection dynamics. In Section 3 we analyse the properties of this model by relying both on simulations and nonlinear bifurcation analysis. Finally, we discuss the implications and limitations of the proposed model in Section 4.

2 Apoptosis-compliant model for the HIV infection dynamics

Section 2.1 briefly describes the model of Adams *et al.* introduced in [7]. On the basis of this model, we propose in Section 2.2 an extension which takes into account the activation-induced apoptosis phenomenon.

2.1 The model of Adams et al.

The model of Adams *et al.* introduced in [7] is a compartmental ODE model in which each compartment corresponds to a specific type of cell population. The model predicts the time evolution of specific cell populations such as, for example, blood concentrations of $CD4^+$ T-lymphocytes and plasma concentration of HIV virions. More specifically, it is described by the following set of ODEs

$$\dot{T}_1 = \lambda_1 - d_1 T_1 - k_1 V T_1 \tag{1}$$

$$\dot{T}_2 = \lambda_2 - d_2 T_2 - k_2 V T_2 \tag{2}$$

$$\dot{T}_1^* = k_1 V T_1 - \delta T_1^* - m_1 E T_1^* \tag{3}$$

$$\dot{T}_2^* = k_2 V T_2 - \delta T_2^* - m_2 E T_2^* \tag{4}$$

$$\dot{V} = N_T \delta \left(T_1^* + T_2^*\right) - cV - \left(\rho_1 k_1 T_1 + \rho_2 k_2 T_2\right) V \tag{5}$$

$$\dot{E} = \lambda_E + \frac{b_E \left(T_1^* + T_2^*\right)}{\left(T_1^* + T_2^*\right) + K_b} E - \frac{d_E \left(T_1^* + T_2^*\right)}{\left(T_1^* + T_2^*\right) + K_d} E - \delta_E E \tag{6}$$

where T_1 (T_1^*) denotes the number of non-infected (infected) $CD4^+$ T-lymphocytes (in cells/ml), T_2 (T_2^*) the number of non-infected (infected) macrophages (in cells/ml), V the number of free HIVs (in virions/ml) and E the number of HIV-specific cytotoxic $CD8^+$ T-cells (in cells/ml). The model proposed in [7] also includes two control inputs representing the effect of the two main types of drugs (protease inhibitors and reverse transcriptase inhibitors) typically used in highly active anti-retroviral therapy. In this paper, we specifically focus on the mathematical modelisation of activation-induced apoptosis for non-treated patients and therefore do not consider these two control inputs.

The values of the different parameters of the model are taken from [7]: $\lambda_1 = 10,000$ [cells/(ml × day)], $d_1 = 0.01$ (1/day), $k_1 = 8 \times 10^{-7}$ [ml/(virions × day)], $\lambda_2 = 31.98$ [cells/(ml × day)], $d_2 = 0.01$ (1/day), $f = 0.34$, $k_2 = 10^{-4}$ [ml/(virions × day)], $\delta = 0.7$ (1/day), $m_1 = 10^{-5}$ [ml/(cells × day)], $m_2 = 10^{-5}$ [ml/(cells × day)], $N_T = 100$ (virions/cells), $c = 13$ (1/day), $\rho_1 = 1$ (virions/cells), $\rho_2 = 1$ (virions/cells), $\lambda_E = 1$ [cells/(ml × day)], $b_E = 0.3$ (1/day), $K_b = 100$ (cells/ml), $d_E = 0.25$ (1/day), $K_d = 500$ (cells/ml), and $\delta_E = 0.1$ (1/day).

As a general remark, some side simulations have shown that all the results presented in this paper are qualitatively robust with respect to perturbations of the nominal parameter values listed above. We therefore only consider these nominal values in the presented results.

In order to provide insight into the properties of this model, we briefly discuss its main characteristics.

As shown in [7], the system of ODEs (1)–(6) exhibits four physical equilibrium points (and several non-physical ones, omitted here, for which one or several state variables are negative). The first three physical equilibrium points have a clear biological interpretation. The fourth equilibrium point has no clear biological interpretation and can be shown to be locally unstable. Nevertheless, this latter equilibrium

point plays an important role in the apoptosis-compliant dynamics as we will discuss later in Section 3.

These physical equilibrium points are, respectively,

1. an uninfected unstable equilibrium point

$$(T_1, T_2, T_1^*, T_2^*, V, E)_{eq} = (10^6, 3198, 0, 0, 0, 10)$$

2. an infected, so-called 'healthy', locally stable equilibrium point

$$(T_1, T_2, T_1^*, T_2^*, V, E)_{eq} = (967839, 621, 76, 6, 415, 353104)$$

which corresponds to a small viral load, a high $CD4^+$ T-lymphocytes count and a high HIV-specific cytotoxic T-cells count;

3. an infected, so-called 'non-healthy', locally stable equilibrium point

$$(T_1, T_2, T_1^*, T_2^*, V, E)_{eq} = (163573, 5, 11945, 46, 63919, 24)$$

for which T-cells are depleted and the viral load is very high;

4. an infected locally unstable equilibrium point

$$(T_1, T_2, T_1^*, T_2^*, V, E)_{eq} = (664938, 50, 1207, 11, 6299, 207658)$$

Numerical simulations show that the basin of attraction of the 'healthy' steady state is relatively small in comparison with the one of the 'non-healthy' steady state. Furthermore, perturbation of the uninfected steady state by adding as less as one single HIV per ml of blood plasma leads to asymptotic convergence towards the 'non-healthy' steady-state as can be seen in Fig. 1.

2.2 Incorporation of the apoptosis phenomenon into the model of Adams et al.

Apoptosis, also called programmed cell death, is a process of deliberate life relinquishment by a cell in a multicellular organism. It is an important biological process whose main goal is to eliminate selected cells for the benefit of the whole organism. Apoptosis can, for example, occur when a cell is damaged beyond repair, infected with a virus, or undergoing stress conditions such as starvation. The 'decision' for apoptosis can either come from the cell itself, or be induced from its surrounding environment (see [13] for a general introduction on apoptosis).

In the special case of lymphocytes, apoptosis plays an important role in optimising the functions of the immune system by compensating lymphocytes proliferation through the elimination of cells that have become ill or ineffective.

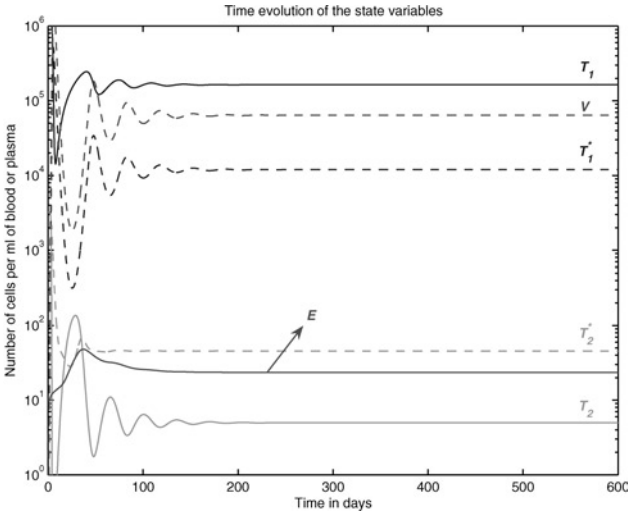

Figure 1 *Time evolution of the state variables of the model (1)–(6) starting from the primo-infection initial condition* $(T_1, T_2, T_1^*, T_2^*, V, E) = (10^6, 3198, 0, 0, 1, 10)$

When apoptosis is not influenced by the presence of other cells, its effect can be considered as constant during the HIV infection, that is, the death rates of the cells related to apoptosis does not change with the evolution of the disease. In such a context, apoptosis is generally included in the natural death rate of each cell [represented by the terms $-d_1 T_1$, $-d_2 T_2$, $-\delta_E E$ and, to a certain extent, $-\delta T_1^*$ and $-\delta T_2^*$ in the model (1)–(6)]. However, this cannot be the case for environment-dependent apoptosis. Indeed, as reported in [1, 4], lymph nodes of HIV-infected individuals contain a high percentage (with respect to uninfected individuals) of uninfected $CD4^+$ and $CD8^+$ cells which are in an apoptotic state – that is which are ready to enter into an apoptotic process. Furthermore, these studies also showed that the apoptosis rates of these apoptotic cells were dependent on the stage of evolution of the HIV infection, and more specifically on the number of infected cells. As a general conclusion of these observations, the per-day proportion of uninfected but apoptotic $CD4^+$ and $CD8^+$ T-cells must be dependent on the number of infected cells and thus cannot be represented by constant factors (d_1, d_2, δ_E or δ) as is the case for spontaneous apoptosis.

From a biological point of view, uninfected $CD4^+$ and $CD8^+$ T-cells have been shown to be prematurely marked for apoptosis because of the presence of biochemical messengers, for example, the glycoprotein gp120, one of the most well-established apoptosis-inducing factor [2, 3]. As summarised in [14, 15], there are several main potential sources for apoptosis-inducing factors: infected cells or free virus particles expressing gp120 on their surface, soluble gp120 alone and Tat viral proteins. Other viral proteins, such as the accessory protein Nef [16] and possibly the immediate-early protein Vpr [17] may also induce apoptosis. Furthermore, some references [2] suggest the

doi: 10.1049/iet-syb:20070029

existence of a two-step mechanism in which, first, T-cells are primed for a premature death by interaction with gp120, and secondly, the actual death signal is delivered by membrane-bound TNF-alpha on the surface of macrophages.

For the sake of obtaining a model which is able to qualitatively capture the activation-induced apoptosis phenomenon without becoming too complex for its analysis, we assume that all the potential apoptosis-inducing factors are directly correlated with the concentration of HIV-infected $CD4^+$ T-cells (T_1^*) and that the activation-induced apoptosis signalling does not involve macrophages. Finally, we assume that the per-day apoptosis proportions depend linearly on the concentration of infected $CD4^+$ T-cells. It would also, for example, make sense to consider that the infected $CD4^+$ T-cells, macrophages and free HIV are correlated with the apoptosis-inducing factors. However, some side simulations and analysis not reported in this paper, have shown that replacing the term $a_{T_1}T_1^*$ by the term $a_{T_1}(\alpha T_1^* + \beta T_2^* + (1-\alpha-\beta)V)$ with $\alpha, \beta \in [0, 1]$ and $\alpha + \beta = 1$ yields results which are qualitatively quite similar. This can be explained by the fact that the time evolutions of infected $CD4^+$ T-cells, macrophages and virions predicted by our model are highly correlated. The main reason for having adopted the simpler term $a_{T_1}T_1^*$ was to obtain a model which could capture the fundamental dynamics associated with the activation-induced apoptosis phenomenon, while, at the same time, being simple enough to lend itself to a detailed analysis.

Consequently, we propose the following modification of the non-infected $CD4^+$ T-cells dynamics: $\dot{T}_1 = \lambda_1 - d_1T_1 - k_1VT_1 - \delta_{T_1}T_1$ where δ_{T_1} (expressed in 1/day) denotes the activation-induced apoptosis proportion of non-infected $CD4^+$ T-cells. According to our previously described assumptions, we assume that δ_{T_1} depends solely on T_1^*, that is, $\dot{T}_1 = \lambda_1 - d_1T_1 - k_1VT_1 - \delta_{T_1}(T_1^*)T_1$. Finally, assuming this dependence on T_1^* to be linear, we obtain that $\delta_{T_1}(T_1^*) = a_{T_1}T_1^*$ where a_{T_1} is a non-negative parameter [expressed in ml/(cells × day)] called the activation-induced apoptosis parameter of uninfected $CD4^+$ T-cells when in presence of infected $CD4^+$ T-cells (or apoptosis parameter for short). A similar modification is considered for the dynamics of $CD8^+$ cells. The corresponding modified model writes

$$\dot{T}_1 = \lambda_1 - d_1T_1 - k_1VT_1 - a_{T_1}T_1^*T_1 \quad (7)$$

$$\dot{T}_2 = \lambda_2 - d_2T_2 - k_2VT_2 \quad (8)$$

$$\dot{T}_1^* = k_1VT_1 - \delta T_1^* - m_1ET_1^* \quad (9)$$

$$\dot{T}_2^* = k_2VT_2 - \delta T_2^* - m_2ET_2^* \quad (10)$$

$$\dot{V} = N_T\delta(T_1^* + T_2^*) - cV - (\rho_1k_1T_1 + \rho_2k_2T_2)V \quad (11)$$

$$\dot{E} = \lambda_E + \frac{b_E(T_1^* + T_2^*)}{(T_1^* + T_2^*) + K_b}E - \frac{d_E(T_1^* + T_2^*)}{(T_1^* + T_2^*) + K_d}E - \delta_E E - a_E T_1^* E \quad (12)$$

where a_{T_1} and a_E are expressed in ml/(cells × day).

3 Analysis of the apoptosis-compliant model

In this section, we analyse the HIV infection dynamics model described by the system of ODEs (7)–(12). This analysis mainly focuses on the study of the influence of the apoptosis parameters a_{T_1} and a_E on the modelled dynamics.

In order to study the influence of some parameters on the dynamics of a nonlinear system modelled by ODEs, one generally relies on a combination of two complementary approaches. The first one is a simulation-based approach which consists in numerically integrating the set of ODEs for different values of the system parameters (and often also for different initial conditions). The second one is more analytical and relies on a bifurcation analysis of the system with respect to the parameters of interest. This second approach aims at establishing the influence of the parameters of interest on the number, the stability and the position of the attractors of the system.

More specifically, the simulation part allows us to identify typical asymptotic behaviours exhibited by the proposed model and to determine the time needed to reach a specific neighbourhood of these asymptotic behaviours. On the other hand, the bifurcation analysis provides a better insight into the dynamic mechanisms that correlate the apoptosis parameters a_{T_1} and a_E with these asymptotic behaviours.

For the sake of simplicity, the analysis will start by considering that a_E is equal to zero which is equivalent to neglecting activation-induced apoptosis in the dynamics of $CD8^+$ T-cells. Afterwards, we study the case where both a_{T_1} and a_E are different from zero. To lighten the presentation of the results, we will mainly consider in our study a single initial state corresponding to the primo-infection point $(T_1, T_2, T_1^*, T_2^*, V, E) = (10^6, 3198, 0, 0, 1, 10)$ and limit the range of values for a_{T_1} and a_E to [0, 1]. Although this may seem to be restrictive, we found that the qualitative nature of our results were very robust with respect to 'biologically plausible' initial conditions. Furthermore, we believe that for values of a_{T_1} and a_E greater than 1, the modelled activation-induced apoptosis rates become so important that they cannot remain in adequacy with reality. Indeed, such high values of the apoptosis parameters would yield an almost complete depletion of the T-cells within less than a few minutes.

3.1 Simulation results for $a_{T_1} \in [0, 1]$ and $a_E = 0$

By numerically integrating the model (7)–(12) starting from various initial conditions for different values of $a_{T_1} \in [0, 1]$, we have always observed convergence to an equilibrium point. However, the position of this equilibrium was found to be highly dependent on the value of the apoptosis parameter a_{T_1}. For $0 \leq a_{T_1} \leq 3.874 \times 10^{-5}$, this position evolves continuously when the values of a_{T_1} are increased, and remains very close to the position of the 'non-healthy' equilibrium point corresponding to $a_{T_1} = 0$. At the particular threshold value $a_{T_1} = 3.874 \times 10^{-5}$, there is a sudden 'jump' towards a new position for which the corresponding asymptotic values of the state variables can be associated to a healthier situation, that is, the viral load and infected cells concentrations are drastically decreased, whereas the non-infected and HIV-specific cytotoxic T-cells concentrations are significantly increased. However, beyond the threshold value $a_{T_1} = 3.874 \times 10^{-5}$, this previously described healthier situation steadily degrades with increasing values of a_{T_1}. For values of a_{T_1} greater than say 10^{-3}, convergence to a point which is 'less healthy' than the 'non-healthy' equilibrium point described in Section 2.1 occurs.

In Fig. 2 we represent three typical time evolutions for the state variables of the model (7)–(12) when starting from the primo-infection point. These three time evolutions correspond to the following apoptosis parameter values $a_{T_1} = 10^{-5}$, $a_{T_1} = 10^{-4}$ and $a_{T_1} = 10^{-2}$, respectively.

Up to this point, we have mainly focused on the study of the properties of the system (7)–(12) in asymptotic conditions. However, as illustrated in Fig. 3, the time needed to reach a close neighbourhood of the asymptotic equilibrium values may be large. Some side simulations have shown that a significant increase in the settling-time values around the bifurcation threshold always occurs independently of the chosen initial condition. Therefore, the results presented in Fig. 3 for the primo-infection initial condition can be considered as representative for any initial condition. In particular, the time needed for the state-space trajectories to reach a neighbourhood of the equilibrium point to which they asymptotically converge is significantly increasing around the threshold value $a_{T_1} = 3.874 \times 10^{-5}$. This latter observation together with the fact that during the transient period the state variables deviation with respect to their asymptotic value may be significant (Fig. 2) show that the transient dynamics and settling time must also be taken into consideration when studying the effects of activation-induced apoptosis.

In order to obtain a better insight into the influence of the apoptosis parameter a_{T_1} on the dynamics of the proposed model, and especially to understand why there exists a range of values for a_{T_1} for which the patient state converges to an equilibrium point which is significantly healthier than the non-healthy equilibrium point described in Section 2, we perform, in Section 3.2, a detailed bifurcation analysis.

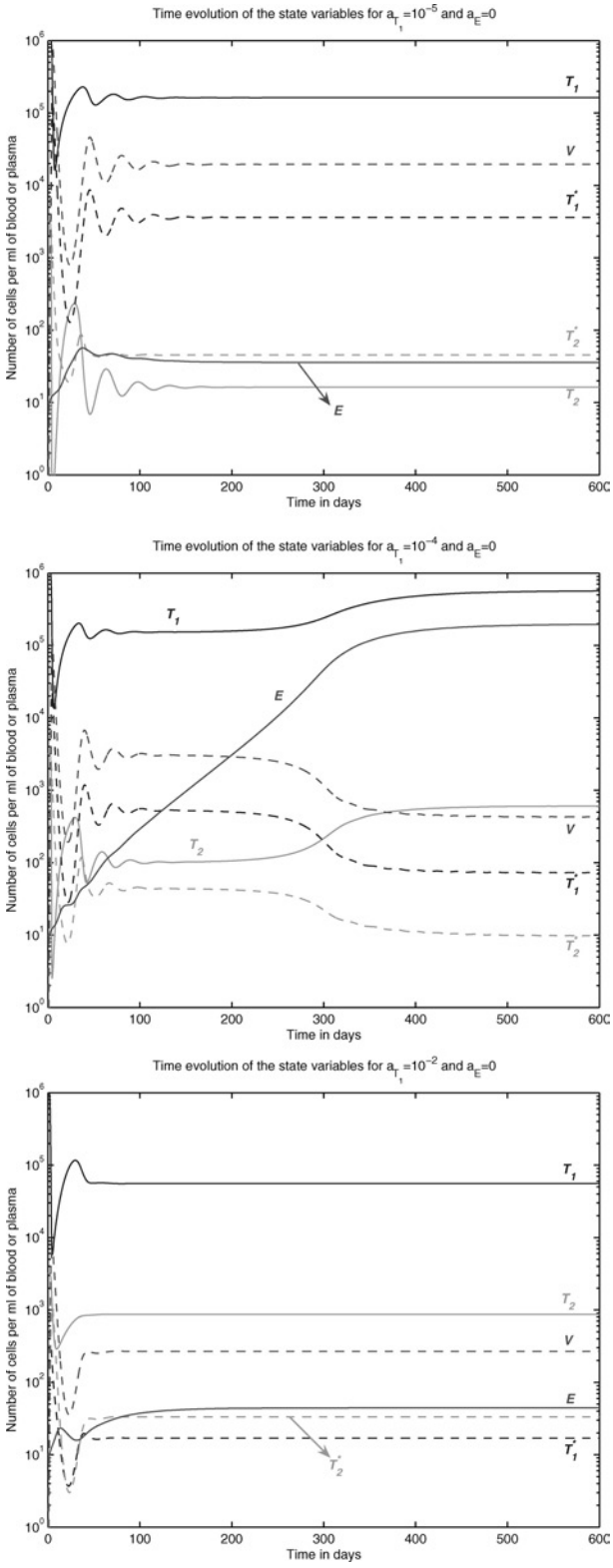

Figure 2 *Time evolution of the state variables of the model (7)–(12) for different values of the apoptosis parameter $a_{T_1} = 10^{-5}$ (top), $a_{T_1} = 10^{-4}$ (middle) and $a_{T_1} = 10^{-2}$ (bottom)*

For every graph, the model has been numerically integrated starting from the primo-infection initial condition (T_1, T_2, T_1^*, T_2^*, V,E) = (10^6, 3198, 0, 0, 1, 10) and the effect of activation-induced apoptosis on the dynamics of the $CD8^+$ T-cells has been neglected (i.e. $a_E = 0$)

doi: 10.1049/iet-syb:20070029

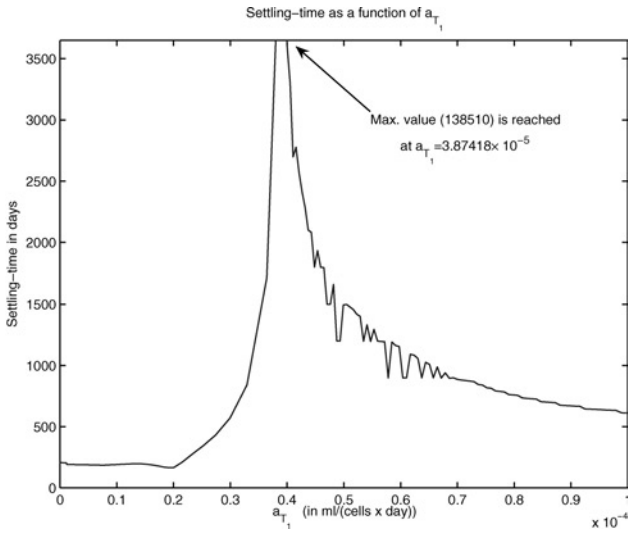

Figure 3 *Evolution of the settling time as a function of the apoptosis parameter a_{T_1}, when starting from the primo-infection initial condition and considering $a_E = 0$*

The settling time is defined as the minimum time required for the state variables to be within an infinite-norm distance of 1% of their asymptotic value.
The maximum settling-time value (138 510 days) is reached at the threshold value $a_{T_1} = 3.87418 \times 10^{-5}$

3.2 Bifurcation analysis for $a_{T_1} \in [0, 1]$ and $a_E = 0$

We performed a bifurcation analysis of the equilibrium points of the model (7)–(12) by relying on the numerical tool MATCONT [18] (MATCONT is a MATLAB toolbox incorporating various numerical differential equation solvers and continuation algorithms for bifurcation analysis. It is freely available at http://www.matcont.ugent.be/). The results of this bifurcation analysis are given in Fig. 4 where the physical infected equilibrium point values of T_1 are represented as a function of the apoptosis parameter a_{T_1}. The unstable uninfected equilibrium point value of T_1 is independent of a_{T_1} and is thus not represented.

This bifurcation diagram helps in understanding the different observed behaviours. For values of a_{T_1} in the range $[0, 3.874 \times 10^{-5}]$, three equilibrium points coexist, two of them are locally stable (eq. point 1 and eq. point 2), whereas the remaining one is unstable. The asymptotic behaviour of the system depends on the chosen initial condition for the model. Performing simulations for a large number of 'biologically plausible' initial conditions, we have always observed convergence to one of the two locally stable equilibrium points. Furthermore, considering $a_{T_1} \in [0, 3.874 \times 10^{-5}]$ and starting from the primo-infection initial condition or a perturbed version of this initial condition convergence to the non-healthy stable equilibrium point (eq. point 2) has always been observed. During the simulations, we have considered perturbations for which the initial concentrations are defined as $(k_1 T_{1_{pi}}, k_2 T_{2_{pi}}, k_3 T^*_{1_{pi}}, k_4 T^*_{2_{pi}}, k_5 V_{pi}, k_6 E_{pi})$ with k_i, $i = 1, \ldots, 6$ randomly chosen in the interval [0.75, 1.25] and $(T_{1_{pi}}, T_{2_{pi}}, T^*_{1_{pi}}, T^*_{2_{pi}}, V_{pi}, E_{pi}) = (10^6, 3198, 0, 0, 1, 10)$. This latter observation confirms that the basin of attraction of the healthy equilibrium point (eq. point 1) is much smaller when compared with the one of the non-healthy equilibrium point (eq. point 2). At $a_{T_1} = 3.874 \times 10^{-5}$, the non-healthy equilibrium point (eq. point 2) coalesces with the unstable one through a saddle-node (also called limit point) bifurcation. We denote this point by LP_1 where LP stands for limit point. For values of a_{T_1} in the range $[3.874 \times 10^{-5}, 1]$, a single locally stable equilibrium point exists (eq. point 1). Furthermore, as a_{T_1} increases towards 1, the position of this locally stable equilibrium (eq. point 1) evolves in such a way that $T_{1_{eq}}$, $T_{2_{eq}}$ and E_{eq} decrease, whereas $T^*_{1_{eq}}$, $T^*_{2_{eq}}$ and V_{eq} increase, explaining the previously simulation-observed degradation in the patient state.

Remark: If one performs a bifurcation analysis for negative values of a_{T_1}, a second saddle-node bifurcation point appears, where eq. point 1 coalesces with the unstable equilibrium point. We denote this point by LP_2. This point LP_2 has not been represented in Fig. 4 since negative values of a_{T_1} make no biological sense in our model. Nevertheless, noting the existence of this second saddle-node bifurcation point is important in order to understand the two-parameter bifurcation analysis presented in Section 3.3.

3.3 Analysis for $a_{T_1} \in [0, 1]$ and $a_E \in [0, 1]$

In this section, we additionally include the effect of activation-induced apoptosis on the $CD8^+$ T-lymphocytes and thus

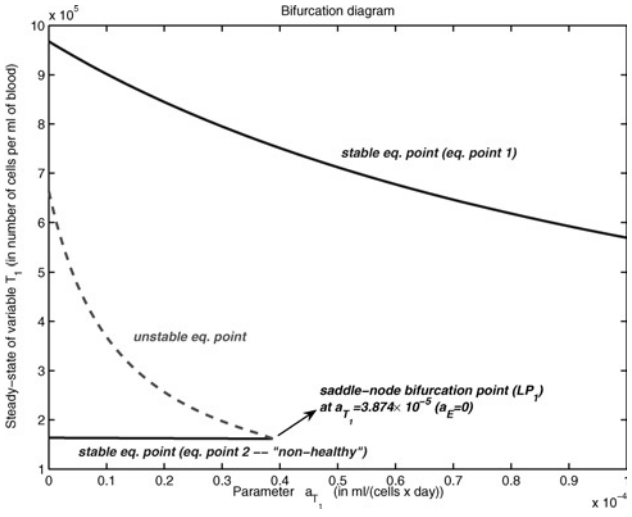

Figure 4 *Bifurcation diagram of the equilibrium concentrations of non-infected $CD4^+$ T-cells ($T_{1_{eq}}$) when the bifurcation parameter a_{T_1} varies from 0 to 10^{-4}.*

A saddle-node bifurcation point (LP_1) exists at $a_{T_1} = 3.874 \times 10^{-5}$. Only the infected equilibrium points (equilibrium points 2, 3 and 4) are represented and a_E is chosen equal to 0. The equilibrium points at $a_{T_1} = 0$ correspond to the three infected equilibrium points of the model (1)–(6) described in Section 2.1

consider the model (7)–(12) where both a_{T_1} and a_E may take non-zero values. We first describe the results of a bifurcation analysis encompassing both the parameters a_{T_1} and a_E. Afterwards, we discuss the additional information that simulations can bring with respect to this analysis. This two-parameter bifurcation analysis is based on a numerical continuation of the saddle-node bifurcation point LP_1 occurring at $\left(a_{T_1}, a_E\right) = \left(3.874 \times 10^{-5}, 0\right)$ (see [19, 20] for details about the continuation algorithm used). The corresponding two-parameter continuation diagram is given in Fig. 5. In this latter figure, we can see that a CUSP bifurcation point exists at $\left(a_{T_1}, a_E\right) = \left(4.838 \times 10^{-4}, 1.956 \times 10^{-4}\right)$, (At the CUSP bifurcation point, two branches of saddle-node bifurcation curves meet tangentially. For nearby parameter values, the system can have three equilibria which collide and disappear pairwise via the saddle-node bifurcations.) At this point, two branches, LP_1 and LP_2, of saddle-node bifurcation curves meet tangentially. These two branches divide the parameter plane into two regions. Inside the wedge between LP_1 and LP_2, there are three equilibria, two stable (eq. points 1 and 2) and one unstable. Outside the wedge, there is a single equilibrium, which is stable. This equilibrium point may be either eq. point 1 or eq. point 2 depending if we are below LP_1 or above LP_2. If we approach the CUSP point from inside the LP_1–LP_2 wedge, all three equilibria merge together so that only a single stable equilibrium point remains beyond the CUSP bifurcation point.

To obtain a clear understanding of the influence of the two activation-induced apoptosis parameters a_{T_1} and a_E on the set of reached equilibrium points when starting from the primo-infection initial condition we consider the 3D plot given in Fig. 6.

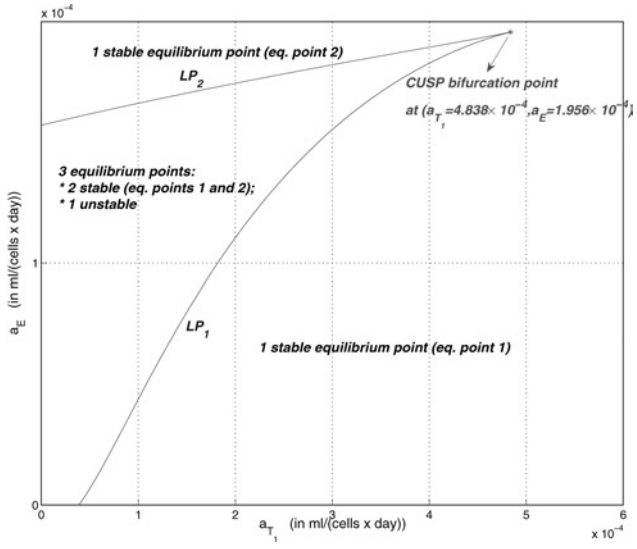

Figure 5 *Two-parameter continuation of the saddle-node bifurcation point LP_1 corresponding to $(a_{T_1}, a_E) = (3.87418 \times 10^{-5}, 0)$.*

A CUSP bifurcation point appears at $(a_{T_1}, a_E) = (4.838 \times 10^{-4}, 1.956 \times 10^{-4})$.

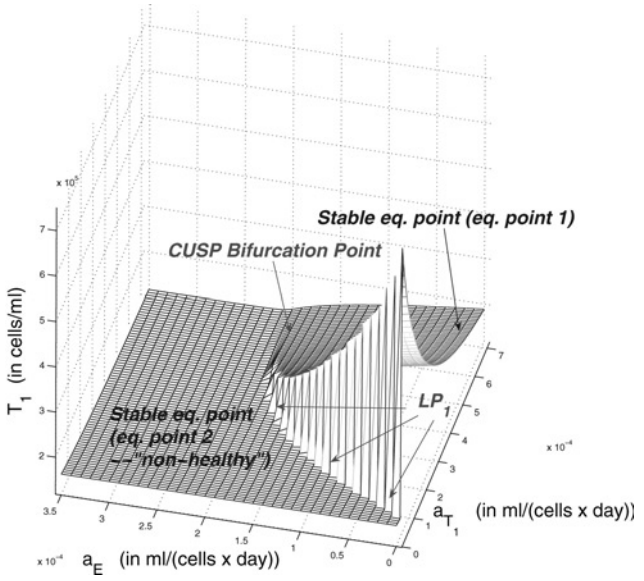

Figure 6 *Concentrations of non-infected CD4$^+$ T-cells (T_1) corresponding to the equilibrium point to which the patient's state converges when starting from the primo-infection initial condition.*

The saddle-node bifurcation curve LP_2 is not visible since starting from the primo-infection initial condition all trajectories corresponding to (a_{T_1}, a_E)-values inside the LP_1–LP_2 wedge converge to the 'non-healthy' stable equilibrium point (eq. point 2)

Fig. 6 represents for different values of $\left(a_{T_1}, a_E\right)$ the value of T_1 corresponding to the equilibrium point to which the patient's state converges when starting from the primo-infection initial condition. Similar to what we observed in Section 3.2, we see that there exist ranges of values of a_{T_1} and a_E where activation-induced apoptosis can have a beneficial effect that hinders the progression of the HIV infection. These values are located below the LP_1 curve in the $\left(a_{T_1}, a_E\right)$-plane (Fig. 5). For any fixed value of a_E in the range $[0, 1.956 \times 10^{-4}]$, by increasing the value of a_{T_1} just above the corresponding threshold value defined by the LP_1 curve, there is a sudden change in the value of T_1 associated with the convergence point. This is due to the fact that below the LP_1 curve given in Fig. 5, the system converges to an equilibrium point parented with the healthy equilibrium point (eq. point 1), as defined in Section 3.1, while above this curve it converges to a point parented with the non-healthy equilibrium (eq. point 2). Increasing the value of a_{T_1} further beyond this LP_1-defined threshold value, the 'healthiness' (measured in proportion with the corresponding value of $T_{1_{eq}}$) of the convergence point decreases with increasing values of a_{T_1}. It is also important to note that for any value of a_{T_1}, the healthiness of the convergence point always decreases with a_E. These two parameters do not have the same effect on the HIV infection as can be seen from the asymmetry of the graphs given in Figs. 5 and 6. Actually, this can be explained by the fact that the death of CD4$^+$ T-cells by the activation-induced apoptosis can mitigate the HIV infection by limiting the number of cells in which the HIV can copy itself, whereas this is not the case for CD8$^+$ T-cells since they are not

doi: 10.1049/iet-syb:20070029

directly targeted by HIVs in our model. Also, and similar to what we showed in Section 3.1, we found that the settling time, that is, the time needed to reach a small neighbourhood of the asymptotically reached equilibrium point, becomes particularly large for $\left(a_{T_1}, a_E\right)$ values located close to the LP_1 curve.

4 Discussion

On the basis of the HIV infection dynamics model proposed by Adams in [7], we have proposed an extended model which aims at incorporating the apoptosis-inducing effects that the HIV infection has on non-infected $CD4^+$ and $CD8^+$ T-cells.

The part of this model specific to these activation-induced apoptosis phenomena depends upon two apoptosis parameters which determine its magnitude (a_{T_1} and a_E). Using a combination of numerical simulations and bifurcation analysis, we found that for some ranges of values of these parameters, these activation-induced apoptosis phenomena could have some beneficial effects on the control of the HIV infection. Indeed, in those ranges, the effect of activation-induced apoptosis modifies the time evolution of the $CD4^+$ T-cells concentrations in a way which is particularly beneficial for preserving the immune system integrity. On the other hand, when the magnitude of the apoptosis parameters becomes too large, this potential beneficial effect disappears and the activation-induced apoptosis mechanisms were then found to aggravate the HIV infection. Furthermore, since the HIV infection worsens when these activation-induced apoptosis rates become too large, one could also relate the progression of the HIV infection to AIDS to a change of magnitude in these rates. These findings need to be taken with caution since they are dependent on several modelling assumptions (per-day apoptosis proportions are linearly proportional to the concentration of infected $CD4^+$ cells and the propensity non-infected $CD4^+$ and $CD8^+$ cells have to undergo apoptosis is proportional to their concentration) that would certainly require careful experimental validation.

We emphasise that these results could also potentially help in designing new anti-HIV therapies based on a drug-mediated regulation of the activation-induced apoptosis factors (such as gp120) in HIV-infected patients. These therapies could be based on the injection of some specific interleukins to HIV positive patients, such as for example IL-2, IL-7 and IL-15. Interleukins are a group of cytokines (secreted signalling molecules) that are used for ensuring communication between cells. The functions of the immune system strongly depend on interleukins as they provide means of communication (and thus of collaboration) between the different groups of immune system cells. Indeed, the anti-apoptotic effect of these interleukins has been reported in the literature [6, 14, 21]. For example, Ahr *et al.* [14] suggest that IL-15 could be used as an immunorestorative agent in HIV treatment because of its anti-apoptotic properties, and its role in enhancing survival and functions of $CD8^+$ T-cells. Also, the *in vitro* results presented in [6] highlight the beneficial anti-apoptotic effects of IL-2 and IL-7 on $CD4^+$ and $CD8^+$ T-cells of HIV-infected patients. However, the role of interleukins on the immune system of HIV-infected patients/macaques is still a controversial issue since other studies [22] have shown that they could have a detrimental effect. Nevertheless, these contradictory results concerning the effects of interleukins on the HIV infection could potentially be explained by the analysis of our extended model, which shows that a decrease in apoptosis rates does not necessarily lead to a better immune system response.

Finally, we acknowledge that the model proposed in this paper possesses some limitations. In particular, similar to the model initially proposed by Adams *et al.*, our model is not able to predict the *in vivo* observed long-term collapse of the immune system, which may be due to several factors such as virus mutations, or fatigue of the immune system resulting in progressive thymus degradation. In ongoing research, we investigate some modifications of the proposed model to overcome these limitations. Also, our model does not encompass the effects of highly active anti-retroviral drugs and of activation-induced apoptosis on the HIV dynamics. More research would certainly be useful to explore ways to design models that overcome these two limitations.

5 References

[1] PANTALEO G., FAUCI A.S.: 'Apoptosis in HIV infection', *Nat. Med.*, 1995, **1**, (2), pp. 118–120

[2] HERBEIN G., MAHLKNECHT U., BATLIWALLA F., *ET AL.*: 'Apoptosis of CD8+ T cells is mediated by macrophages through interaction of HIV gp120 with chemokine receptor CXCR4', *Nature*, 1998, **395**, (6698), pp. 189–194

[3] GOUGEON M.-L., MONTAGNIER L.: 'Programmed cell death as a mechanism of CD4 and CD8 T cell depletion in AIDS: molecular control and effect of highly active anti-retroviral therapy', *Ann. New York Acad. Sci.*, 1999, **887**, (1), pp. 199–212

[4] BADLEY A.D.: 'Cell death during HIV infection' (CRC Press, 2005)

[5] YUE F.Y., KOVACS C.M., DIMAYUGA R.C., *ET AL.*: 'Preferential apoptosis of HIV-1-specific CD4+ T cells', *J. Immunology*, 2005, **174**, (4), pp. 2196–2204

[6] VASSENA L., PROSCHAN M., FAUCI A.S., LUSSO P.: 'Interleukin 7 reduces the levels of spontaneous apoptosis in CD4+ and CD8+ T cells from HIV-1-infected individuals', *Proc. Natl. Acad. Sci. USA*, 2007, **104**, (7), pp. 2355–60

[7] ADAMS B., BANKS H., KWON H.-D., TRAN H.: 'Dynamic multidrug therapies for HIV: optimal and STI control approaches', *Math. Biosci. Eng.*, 2004, **1**, (2), pp. 223–241

[8] PERELSON A.S., ESSUNGER P., CAO Y., *ET AL.*: 'Decay characteristics of HIV-1-infected compartments during combination therapy', *Nature*, 1997, **387**, pp. 188–191

[9] PERELSON A.S., NELSON P.W.: 'Mathematical analysis of HIV-1 dynamics in vivo', *SIAM Rev.*, 1999, **41**, pp. 3–44

[10] BAJARIA S., WEBB G., KIRSCHNER D.: 'Predicting differential responses to structured treatment interruptions during HAART', *Bull. Math. Biol.*, 2004, **66**, (5), pp. 1093–1118

[11] CHEN J., ZHANG J.-T., WU H.: 'Discretization approach and nonparametric modeling for long-term HIV dynamic model'. Computational Science and Its Applications – ICCSA 2005, 2005 Lecture Notes in Computer Science, (Springer Verlag, Berlin/Heidelberg), vol. 3483, pp. 519–527

[12] GE S., TIAN Z., LEE T.H.: 'Nonlinear control of a dynamic model of HIV-1', *IEEE Trans. Biomed. Eng.*, 2005, **52**, (3), pp. 353–361

[13] LAWEN A.: 'Apoptosis-an introduction'. BioEssays: news and reviews in molecular, cellular and developmental biology, Sepember 2003, vol. 25, pp. 888–96 pMID: 12938178

[14] AHR B., ROBERT-HEBMANN V., DEVAUX C., BIARD-PIECHACZYK M.: 'Apoptosis of uninfected cells induced by HIV envelope glycoproteins', *Retrovirology*, 2004, **1**, p. 12, pMID: 15214962

[15] WANG J., GUAN E., RODERIQUEZ G., NORCROSS M.A.: 'Synergistic induction of apoptosis in primary CD4+ T cells by macrophage-tropic HIV-1 and TGF-beta1', *J. Immunology*, 2001, **167**, pp. 3360–3366

[16] ZAULI G., GIBELLINI D., SECCHIERO P., *ET AL.*: 'Human immunodeficiency virus Type 1 Nef protein sensitizes CD4+ T lymphoid cells to apoptosis via functional upregulation of the CD95/CD95 ligand pathway', *Blood*, 1999, **93**, pp. 1000–1010

[17] STEWART S.A., POON B., SONG J.Y., CHEN I.S.Y.: 'Human immunodeficiency virus Type 1 Vpr induces apoptosis through caspase activation', *J. Virology*, 2000, **74**, pp. 3105–3111

[18] DHOOGE A., GOVAERTS W., KUZNETSOV Y.: 'Matcont: a MATLAB package for numerical bifurcation analysis of ODEs', *ACM Trans. Math. Softw.*, 2003, **29**, pp. 141–164

[19] KHIBNIK A., KUZNETSOV Y., LEVITIN V., NIKOLAEV E.: 'Continuation techniques and interactive software for bifurcation analysis of ODEs and iterated maps', *Physica D*, 1993, **62**, pp. 360–371

[20] DOEDEL E., GOVAERTS W., KUZNETSOV Y., DHOOGE A.: 'Numerical continuation of branch points of equilibria and periodic orbits', *Int. J. Bifurcation Chaos*, 2005, **15**, pp. 841–860

[21] BEQ S., DELFRAISSY J.-F., THEZE J.: 'Interleukin-7 (IL-7): immune function, involvement in the pathogenesis of HIV infection and therapeutic potential', *Eur. Cytokine Netw.*, 2004, **15**, (4), pp. 279–289

[22] FLUUR C., MILITO A.D., FRY T.J., *ET AL.*: 'Potential role for IL-7 in Fas-mediated T cell apoptosis during HIV infection', *J. Immunology*, 2007, **178**, pp. 5340–5350

doi: 10.1049/iet-syb:20070029